Photoinduced Electron Transfer Processes in 1,8-Naphthalimide-Linker-Phenothiazine Dyads

ARTICLE *in* THE JOURNAL OF PHYSICAL CHEMISTRY B · JULY 2006

Impact Factor: 3.3 · DOI: 10.1021/jp057557r · Source: PubMed

6 AUTHORS, INCLUDING:

Dae Won Cho
Korea University
106 PUBLICATIONS **1,401** CITATIONS
SEE PROFILE

Ung Chan Yoon
Pusan National University
130 PUBLICATIONS **1,820** CITATIONS
SEE PROFILE

Photoinduced Electron Transfer Processes in 1,8-Naphthalimide-Linker-Phenothiazine Dyads

Dae Won Cho,[†,‡] Mamoru Fujitsuka,[‡] Akira Sugimoto,[‡] Ung Chan Yoon,[§] Patrick S. Mariano,[#] and Tetsuro Majima*[,‡]

The Institute of Scientific and Industrial Research (SANKEN), Osaka University, Mihogaoka 8-1, Ibaraki, Osaka 567-0047, Japan, Department of Chemistry and the Chemistry Institute for Functional Materials, Pusan National University, Pusan 609-735, Korea, and Department of Chemistry, University of New Mexico, Albuquerque, New Mexico 87131

Received: December 29, 2005; In Final Form: March 15, 2006

Photoinduced electron transfer (PET) processes of 1,8-naphthalimide-linker-phenothiazine (NI-L-PTZ) dyads have been investigated using the nanosecond- and picosecond-transient absorption measurements. Two kinds of linker were introduced, i.e., polymethylene-linked dyad (NI-C8-PTZ and NI-C11-PTZ) and a poly(ethyl ether)-linked one (NI-O-PTZ). The 355 nm pulsed laser excitation of NI-C8-PTZ, NI-C11-PTZ, and NI-O-PTZ in acetonitrile produced NI radical anion ($NI^{\bullet -}$) and PTZ radical cation ($PTZ^{\bullet +}$) with the absorption bands around 420 and 520 nm, respectively, through charge transfer from PTZ to NI in the singlet excited state ($NI(S_1)$) as well as in the triplet excited states ($NI(T_1)$) in acetonitrile. On the other hand, the charge transfer process occurred only from $NI(S_1)$ in nonpolar solvents. The rates of charge transfer and charge recombination processes largely depended on the solvent polarity and they are affected by the length of linkers and electronic coupling through polyether linker. The PET mechanism is discussed in terms of the free energy change for the charge transfer.

Introduction

Photoinduced electron transfer (PET) has been attracting a great deal of attention for several decades because of its importance in wide fields including natural processes such as photosynthesis. The covalently linked dyads of electron donor and acceptor are often used to mimic the electron transfer processes in natural systems.[1−3] The linker connecting donor and acceptor is known to play a critical role in determining the electron transfer rate, because the electron transfer rate is affected by the properties of the linker such as the donor−acceptor distance and the energy matching between the donor and linker components.[4,5]

Phthalimides are well-known as an electron acceptor to undergo the PET reactions with olefins, amines, and electron-rich alkyl benzenes, to produce the corresponding radical anions which subsequently abstract protons from either the solvent or quencher.[6] In our recent efforts, we uncovered PET-induced photocyclization reactions of trimethylsilyl terminated polyheteroatom donor-linked phthalimides. These reactions are proven to be highly efficient methods to construct polyethers, -thioethers, and -sulfonamides[7] and cyclic peptides.[8]

Furthermore, the photochemical properties of naphthalimide are of special interest because they can cause cleavage of oligonucleotides. Saito et al.[9] demonstrated photoinduced DNA cleavage via electron transfer between a guanine base and 1,8-naphthalimide (NI). Recently, we established the mechanism of the photosensitized one-electron oxidation of DNA of the NI derivatives.[10,11] Usually, the PET processes in covalently linked dyads and triads with electron donor molecules have been investigated in aqueous or polar solvents.[3,12−14] However, the PET reactions of NIs have not been fully explored in aprotic polar and nonpolar solvents. Furthermore, the effect of the linker in the PET of NI is still unknown.

In the present study, we have prepared a series of well-designed dyad molecules, in which three kinds of linkers (L) between the electron-donating phenothiazine (PTZ) and the electron-accepting NI moieties were examined, i.e., NI-L-PTZ such as NI-C8-PTZ, NI-C11-PTZ, and NI-O-PTZ (Chart 1), where L is octyl (C8), undecyl (C11), and trioxaundecyl (O), respectively. The reference NI molecules (NI-C1, NI-C7, and NI-O) were also synthesized, as shown in Chart 1. We have examined the solvent effects on the PET processes of the NI-L-PTZ and NI-L and demonstrated the relative roles of the singlet and triplet excited states of NIs in their PET process. We have also found the specific interaction of NI in the singlet excited state with toluene used the solvent.

Experimental Section

Materials. The detail synthesis of the dyads (*N*-(8-phenothiazinyloctyl)-1,8-naphthalimide (NI-C8-PTZ), *N*-(11-phenothiazinylundecyl)-1,8-naphthalimide (NI-C11-PTZ), *N*-(11-phenothiazinyl-3,6,9-trioxaundecyl)-1,8-naphthalimide (NI-O-PTZ)), and reference NI molecules (*N*-methyl-1,8-naphthalimide (**NI-C1**), *N*-heptyl-1,8-naphthalimide (**NI-C7**), *N*-(2-methoxyethyl)-1,8-naphthalimide (**NI-O**)) have been described earlier.[15]

Spectrosocpic Measurements. Nanosecond transient absorption measurements were carried out by employing the technique of laser flash photolysis. The third harmonic generation (THG,

* To whom correspondence should be addressed. Tel: Japan +6-6879-8495. Fax: Japan +6-6879-8499. E-mail: majima@sanken.osaka-u.ac.jp.
[†] Present address: Department of Chemistry, Chosun University, Gwangju 501-759, Korea.
[‡] Osaka University.
[§] Pusan National University.
[#] University of New Mexico.

10.1021/jp057557r CCC: $33.50
Published on Web 05/20/2006

CHART 1

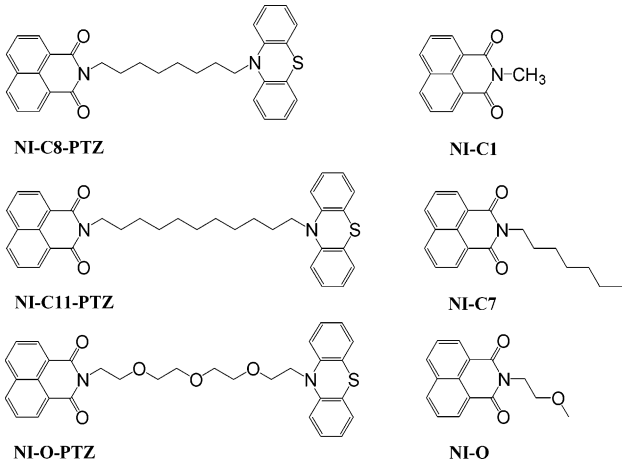

355 nm) of Q-switched Nd:YAG laser (Brilliant, pulse width of 5 ns fwhm) was used to excite the NI moiety selectively, because it has a strong absorption around 355 nm, whereas PTZ has no absorption at wavelengths longer than 320 nm. The pulse energy was ca. 18 mJ pulse^{-1}. A Xenon flash lamp (Osram, XBO-450) was focused into the sample solution as the probe light for the transient absorption measurement. Transient absorption and temporal profiles were measured with a monochromator (Nikon, G250) equipped with a photomultiplier (Hamamatsu Photonics, R928) and a digital oscilloscope (Tektronix, TDS-580D). Reported signals were averages of four events. All solutions were argon-saturated unless otherwise indicated.

Transient absorption spectra in the picosecond region were measured by employing the THG (355 nm) of a picosecond Nd:YAG laser (Continuum, RGA69-10LD, fwhm 30 ps, 20 mJ pulse^{-1}) as an excitation source.[16] Probe light generated by focusing the fundamental light of the Nd:YAG laser on a Xe gas cell was detected with a streak camera (Hamamatsu Photonics, C7700) equipped with a polychromator (Hamamatsu Photonics, C5094) after passing through the sample (Optical path: 5.0 mm).

Time-resolved fluorescence spectra were measured by the single photon counting method,[17] using a streakscope (Hamamatsu Photonics, C4334-01) equipped with a polychromator (Acton Research, SpectraPro150). An ultrashort laser pulse was generated with a Ti:sapphire laser (Spectra-Physics, Tsunami 3941-M1BB, fwhm 100 fs) pumped with a diode-pumped solid-state laser (Spectra-Physics, Millennia VIIIs). For excitation of the sample, the output of the Ti:sapphire laser was converted to THG (300 nm) with a harmonic generator (Spectra-Physics, GWU-23FL).

Steady-state UV−vis absorption spectra were recorded with a UV−vis spectrophotometer (Shimadzu, UV-3100) at room temperature. Fluorescence spectra were measured using a Hitachi 850 fluorophotometer. Fluorescence quantum yields (ϕ_f) were estimated using a toluene solution of anthracene as a standard with a known value of $\phi_f = 0.30$.[18]

The quantum yields of the triplet state formation (ϕ_T) were determined by chemical actinometry. A pair of optically matched sample solutions and an acetonitrile solution of benzophenone were subjected to identical laser flash intensities. Plots of ΔA_{470} as a function of the laser intensity were constructed. From the ratio of slopes, along with the known T_1-T_n extinction coefficient of benzophenone (6500 M^{-1} cm^{-1} at 520 nm) in acetonitrile,[19] the extinction coefficients of NI-C1 in the triplet excited state (NI(T_1)) were determined to be 5100 M^{-1} cm^{-1} at 470 nm. We used the intersystem crossing yield (100%) of NI-C1 to establish the extinction coefficient according to the reported one.[20] To evaluate the quantum efficiencies of the electron transfer, the extinction coefficients of 35 000 M^{-1} cm^{-1} for the NI radical anion (NI$^{\bullet-}$), and that of 10 000 M^{-1} cm^{-1} for the PTZ radical cation (PTZ$^{\bullet+}$) are used, respectively.[21,22]

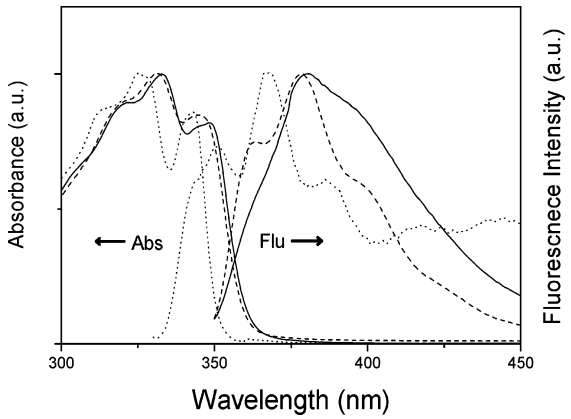

Figure 1. Absorption and fluorescence spectra of NI-C8-PTZ in three solvents: toluene (solid line), acetonitrile (dashed line), and *n*-hexane (dotted line).

Results

Absorption Spectral Properties. The absorption and fluorescence spectra of NI-C8-PTZ in three solvents are shown in Figure 1. Similar absorption and fluorescence spectra were observed for NI-C11-PTZ and NI-O-PTZ in each solvent. Spectroscopic properties are summarized in Table S1 in the Supporting Information. In both acetonitrile and toluene, the absorption bands of NI-L-PTZ at longer wavelengths were observed at 344−348 nm with a peak at 330−333 nm and a shoulder around 320 nm. In *n*-hexane, the absorption spectra of NI-L-PTZ were slightly shifted to the shorter wavelength, showing the absorption maxima at 342 and 327 nm (Figure 1). The absorption spectra of NI-L-PTZ were almost identical to those for other NI derivatives previously reported[20] as well as the reference NI molecules such as NI-C1, NI-C7, and NI-O. This result implies that there is no substantial interaction between NI and PTZ of NI-L-PTZ.

Fluorescence Spectral Properties. The fluorescence maxima of NI-L-PTZ were observed around 378 nm in acetonitrile. In *n*-hexane, the maxima slightly blue-shifted to 367 nm compared to those in acetonitrile. The fluorescence spectra in acetonitrile and *n*-hexane showed a mirror-image relationship with the corresponding absorption spectra. These structured absorption and fluorescence bands indicate that only a narrow distribution of vibrational states is involved in the electronic transition and that the geometry of the molecule in its relaxed excited state is not much different from that in the ground state. Interestingly, although toluene is a nonpolar solvent, the fluorescence spectra of NI derivatives in toluene shifted to longer wavelengths (Table S1, Figure 1) when compared with those in acetonitrile. This result probably indicates the specific interaction between NI in the singlet excited state (NI(S_1)) and toluene to generate the exciplex (see Discussion section).

The ϕ_f values of the reference NI molecules were ∼0.03 in acetonitrile (Table 1), and the values in toluene were similar to those in acetonitrile. On the other hand, those were very small in *n*-hexane. The ϕ_f values were much smaller for NI-L-PTZ than those for the reference NI molecules in all solvents. The fluorescence lifetimes (τ_f) of the reference NI molecules were

TABLE 1: Photophysical Parameters of NI-L-PTZ and Reference NI Molecules in Three Solvents

	in acetonitrile					in toluene			in *n*-hexane[a]	
NI derivative	τ_f (ps)	ϕ_f	ϕ_T	$\phi_{NI^{\bullet-}}$	$\phi_{PTZ^{\bullet+}}$	τ_f (ps)	ϕ_f	ϕ_T	τ_f (ps)	ϕ_f (10^{-3})
NI-C8-PTZ	85	0.011	0	0.16	0.15	133	0.007	0.23	<50	0.13
NI-C11-PTZ	120	0.013	0	0.16	0.13	200	0.008	0.23	<50	0.52
NI-O-PTZ	114	0.016	0	0.07	0.11	160	0.009	0.23	<50	0.25
NI-C1	195	0.027	0.97			351	0.033	0.44	<50	1.8
NI-C7	138	0.021	0.98			236	0.026	0.50	<50	1.9
NI-O	192	0.035	0.96			398	0.039	0.47	<50	2.8

[a] No measurement of ϕ_T was performed, because the absorbance of the NI derivative at 355 nm was smaller than 0.05 even in NI-saturated *n*-hexane solutions. All quantum yields were measured within 5% error. The temporal emission profiles were well fitted into single-exponential function. The residuals were less than 1.1.

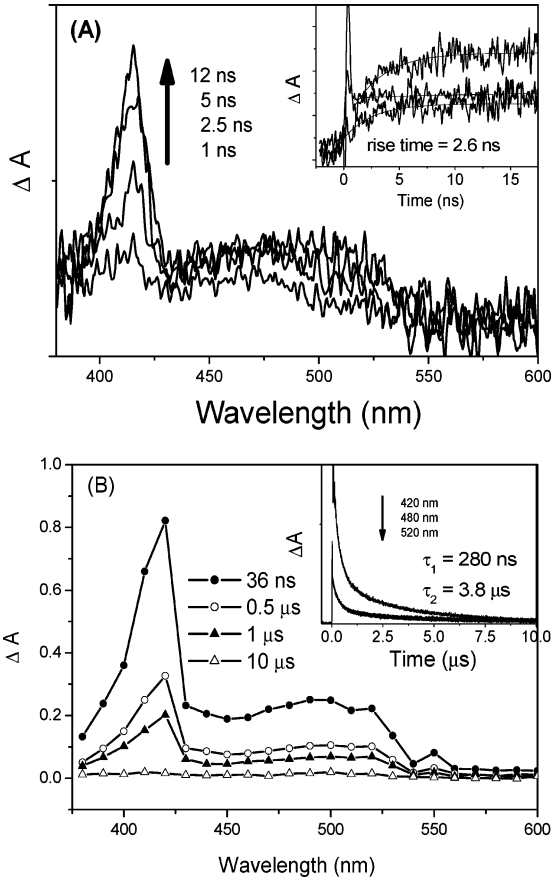

Figure 2. Transient absorption spectra observed at times after 30 ps (A) and 5 ns (B) laser flash during the 355 nm laser flash photolysis of NI-C8-PTZ in acetonitrile. The inset shows kinetic traces of ΔA at 420, 470, and 520 nm. The spike observed immediately after the laser flash is electric noise due to laser flash in the inset (A).

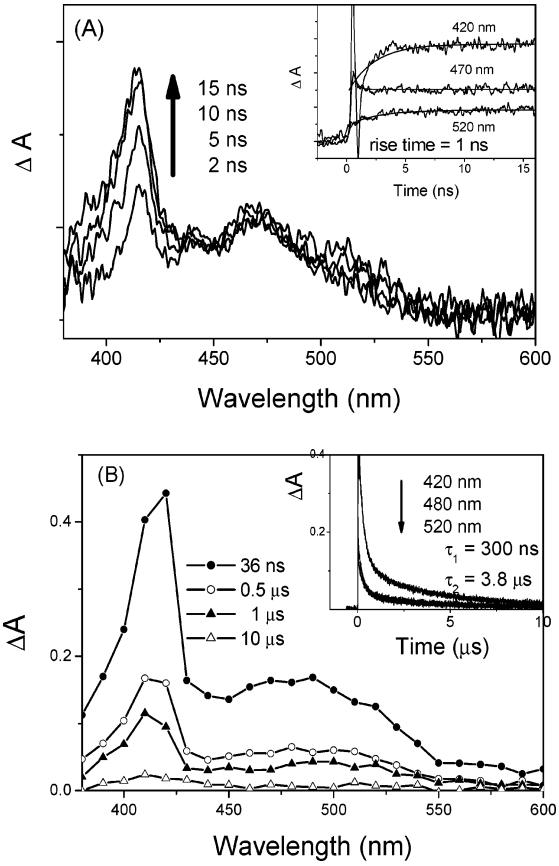

Figure 3. Transient absorption spectra observed at times after 30 ps (A) and 5 ns (B) laser flash during the 355 nm laser flash photolysis of NI-O-PTZ in acetonitrile. The inset shows kinetic traces of ΔA at 420, 470, and 520 nm. The spike observed immediately after the laser flash is electric noise due to laser flash in the inset (A).

measured to be 195, 138, and 192 ps in acetonitrile for NI-C1, NI-C7, and NI-O, respectively, whereas those were 85, 120, and 114 ps for NI-C8-PTZ, NI-C11-PTZ, and NI-O-PTZ, respectively. The τ_f values were shorter for NI-L-PTZ than those of the reference NI molecules. This tendency was confirmed for the τ_f values in toluene. All NI derivatives in *n*-hexane showed the τ_f values of shorter than 50 ps.

Transient Absorption Spectroscopic Properties. Upon excitation of NI-L-PTZ in acetonitrile with a 30 ps duration pulse at 355 nm, two transient absorption bands were observed around 420 and 520 nm (Figures 2 and 3 and Figures S1 and S2 in Supporting Information). These bands can be assigned to $NI^{\bullet-}$ and $PTZ^{\bullet+}$, respectively, according to the previous reports.[12,23,24] These results indicate that the electron transfer process efficiently occurred upon photoexcitation of NI-L-PTZ in acetonitrile. The generation of radical ions by PET is also supported by the fact that the concentrations of $NI^{\bullet-}$ and $PTZ^{\bullet+}$ generated were essentially the same. The quantum yields of $NI^{\bullet-}$ and $PTZ^{\bullet+}$ formation ($\phi_{NI^{\bullet-}}$ and $\phi_{PTZ^{\bullet+}}$) were calculated from the absorbed photon numbers (Table 1). The transient absorption of $NI^{\bullet-}$ at 420 nm and $PTZ^{\bullet+}$ at 520 nm showed growth in the nanosecond time scale. The temporal profiles of the $NI^{\bullet-}$ (420 nm) and $PTZ^{\bullet+}$ (520 nm) transient absorption were analyzed by the first-order rate function with the rate constant (k_{CT}) of 3.8×10^8, 2.6×10^8, and 1.0×10^9 s^{-1} for NI-C8-PTZ, NI-C11-PTZ, and NI-O-PTZ, respectively. These values show that the charge transfer occurred much slower than the fluorescence decay of NI(S_1) in the NI-L-PTZ dyads in acetonitrile. Thus, it is suggested that not only NI(S_1) but also NI(T_1) is involved in the charge transfer process, although no formation of NI(T_1) was observed in acetonitrile. In other words, NI(S_1) undergoes partly the intersystem crossing to give NI(T_1) with competition of the charge transfer process, and NI(T_1) does the charge

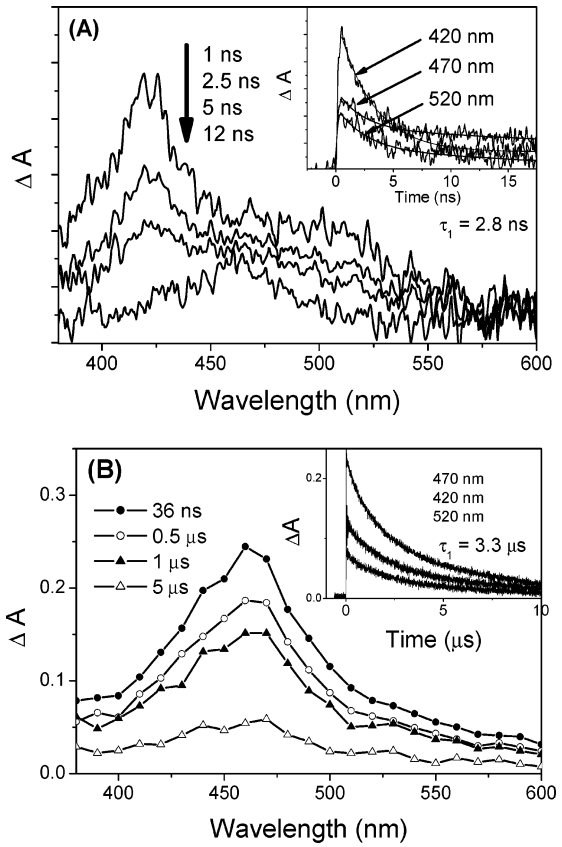

Figure 4. Transient absorption spectra observed at times after 30 ps (A) and 5 ns (B) laser flash during the 355 nm laser flash photolysis of NI-C8-PTZ in toluene. The inset shows kinetic traces of Δ*A* at 420, 470, and 520 nm.

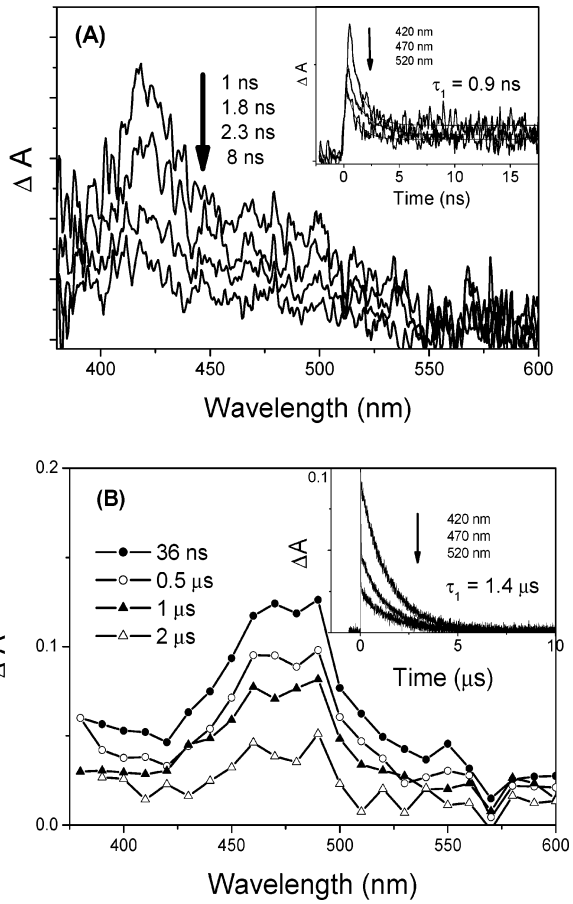

Figure 5. Transient absorption spectra observed at times after 30 ps (A) and 5 ns (B) laser flash during the 355 nm laser flash photolysis of NI-O-PTZ in toluene. The inset shows kinetic traces of Δ*A* at 420, 470, and 520 nm.

transfer process in 100% yield at the rate constant ($k_{CT}(T_1)$) of 3.8×10^8, 2.6×10^8, and 1.0×10^9 s^{-1} for NI(T_1)-C8-PTZ, NI(T_1)-C11-PTZ, and NI(T_1)-O-PTZ, respectively.

The decay profiles of the $NI^{\bullet-}$ and $PTZ^{\bullet+}$ transient absorption of $NI^{\bullet-}$-L-$PTZ^{\bullet+}$ displayed biexponential components, as shown in the insets of Figures 2 and 3. The short-lived and large-amplitude component indicated the decay lifetimes of 280−300 ns and the rate constants (k_{CR}) of 3.3×10^6 to 3.6×10^6 s^{-1}, which are attributed to the intramolecular charge recombination process between $NI^{\bullet-}$ and $PTZ^{\bullet+}$ of $NI^{\bullet-}$-L-$PTZ^{\bullet+}$. In addition, the long-lived component showed the decay lifetimes of 3.8 μs and the apparent rate constants of 2.6×10^5 s^{-1}. The long-lived components could attribute to the intermolecular charge recombination process between the radical ions $NI^{\bullet-}$-L-PTZ and NI-L-$PTZ^{\bullet+}$, generated from the bimolecular charge shift reaction between $NI^{\bullet-}$-L-$PTZ^{\bullet+}$ and NI-L-PTZ.

In toluene, the PET process of NI-L-PTZ has been also investigated with the transient absorption measurements. Immediately after the excitation of NI of NI-L-PTZ with a 355 nm laser pulse with 30 ps duration, the transient absorption bands around 420, 470, and 520 nm were observed (Figures 4 and 5). The 420 and 520 nm absorption bands are assigned to $NI^{\bullet-}$ and $PTZ^{\bullet+}$, respectively, and both bands showed the decay with the time constants of 2.8, 2.0, and 0.9 ns for NI-C8-PTZ, NI-C11-PTZ, and NI-O-PTZ, respectively. The transient absorption band around 470 nm can be assigned to NI(T_1), because this transient band is identical to the T_1-T_n absorption spectra of other NI derivatives reported previously.[3,25] The lifetimes of NI(T_1) in toluene were found to be 3.3, 1.4, and 1.4 μs for NI-C8-PTZ, NI-C11-PTZ, and NI-O-PTZ, respectively.

Upon 355 nm 30 ps laser-pulse excitation of the reference NI molecules (NI-C1, NI-C7, and NI-O), the transient absorption band at 470 nm was observed immediately after the laser pulse and assigned to NI(T_1) and ϕ_T values were ∼0.97 and ∼0.47 in acetonitrile and toluene, respectively. No formation of the transient absorption of $NI^{\bullet-}$ and $PTZ^{\bullet+}$ was observed in both solvents (Figure S3 in Supporting Information).

Discussion

Photodynamic Properties on Photoinduced Electron Transfer in NI-L-PTZ. From the τ_f values, the deactivation rate constants of NI(S_1) in acetonitrile have been determined to be 1.2×10^{10}, 8.3×10^9, and 8.8×10^9 s^{-1} for NI(S_1)-C8-PTZ, NI(S_1)-C11-PTZ, and NI(S_1)-O-PTZ, respectively, which are substantially faster than the deactivation rates of the corresponding reference NI molecules. The ϕ_f values of NI(S_1)-L-PTZ decreased by a factor of 2 in comparison with those of the reference NI molecules. Thus, it is strongly suggested that the diminished fluorescence is attributed to the rapid electron transfer from PTZ to NI(S_1) to give $NI^{\bullet-}$-L-$PTZ^{\bullet+}$. The energy transfer from NI(S_1) to PTZ is not favorable, because the excitation energy of NI(S_1) (3.4 eV) is lower than that of PTZ in the singlet excited state (5.2 eV). On the basis of the difference between the τ_f values of NI(S_1)-L-PTZ and NI(S_1), the charge transfer rate constants (k_{CT}) for NI(S_1)-L-PTZ were determined as shown in Table 2.

No NI(T_1) was observed in NI-L-PTZ, whereas NI(T_1) was produced with ϕ_T ∼0.97 for the reference NI molecules in acetonitrile (Table 1). From the 30 ps transient absorption measurements, the formation rate constants of $NI^{\bullet-}$ and $PTZ^{\bullet+}$ were measured to be 3.8×10^8, 2.6×10^8, and 1.0×10^9 s^{-1}

TABLE 2: Rate Constants of Decays of NI(S_1) and NI(T_1) (k_f and k_T, Respectively), the Charge Transfer of NI-C8-PTZ, NI-C11-PTZ, and NI-O-PTZ in the Singlet and Triplet Excited States ($k_{CT}(S_1)$ and $k_{CT}(T_1)$, Respectively), and the Charge Recombination of $NI^{\bullet-}$-C-$PTZ^{\bullet+}$ and $NI^{\bullet-}$-O-$PTZ^{\bullet+}$ (k_{CR}) in Acetonitrile and Toluene

	rate constants in acetonitrile (s^{-1})					rate constants in toluene (s^{-1})			
NI derivative	k_f	k_T	$k_{CT}(S_1)$[a]	$k_{CT}(T_1)$	k_{CR}	k_f	k_T	$k_{CT}(S_1)$[a]	k_{CR}
NI-C8-PTZ	1.2×10^{10}	–	4.5×10^9	3.8×10^8	3.6×10^6 2.6×10^5	7.5×10^9	2.9×10^5	3.3×10^9	3.6×10^8
NI-C11-PTZ	8.3×10^9	–	1.0×10^9	2.6×10^8	4.4×10^6 3.5×10^5	5.0×10^9	7.2×10^5	8.0×10^8	5.2×10^8
NI-O-PTZ	8.8×10^9	–	3.5×10^9	1.0×10^9	3.3×10^6 2.6×10^5	6.3×10^9	7.4×10^5	3.8×10^9	1.1×10^9
NI-C1	5.1×10^9	3.6×10^5				2.8×10^9	3.1×10^5		
NI-C7	7.3×10^9	3.7×10^5				4.2×10^9	2.9×10^5		
NI-O	5.2×10^9	3.3×10^5				2.5×10^9	2.8×10^5		

[a] The charge transfer rates of NI-L-PTZ in the singlet state were calculated from τ_f of the fluorescence decay according to the following equation, $k_{CT}(S_1) = 1/\tau_{f,NI-C-PTZ} - 1/\tau_{f,NI-C7}$ and $k_{CT}(S_1) = 1/\tau_{f,NI-O-PTZ} - 1/\tau_{f,NI-O}$, respectively. The charge recombination rates of $NI^{\bullet-}$ and $PTZ^{\bullet+}$ for $NI^{\bullet-}$-L-$PTZ^{\bullet+}$ were calculated from the decays of the transient absorption of $NI^{\bullet-}$ and $PTZ^{\bullet+}$. All kinetic constants were established within 5% error.

for NI-C8-PTZ, NI-C11-PTZ, and NI-O-PTZ, in acetonitrile, respectively, indicating that the formation rates are much slower than the fluorescence decay rate of NI(S_1). The generation of $NI^{\bullet-}$ and $PTZ^{\bullet+}$ from the electron transfer from PTZ to NI(T_1) is also possible, as indicated by the free energy change (ΔG_{et}) of the PET, as discussed later. On the basis of the 5 ns laser flash photolysis, the intramolecular charge recombination occurred between $NI^{\bullet-}$ and $PTZ^{\bullet+}$ of $NI^{\bullet-}$-L-$PTZ^{\bullet+}$ at rate constants of 3.6×10^6, 4.4×10^6, and 3.3×10^6 s^{-1} for $NI^{\bullet-}$-C8-$PTZ^{\bullet+}$, $NI^{\bullet-}$-C11-$PTZ^{\bullet+}$, and $NI^{\bullet-}$-O-$PTZ^{\bullet+}$, in acetonitrile, respectively. In addition, much slower charge recombination occurred at the apparent rate constants of 2.6×10^5, 3.5×10^5, and 2.6×10^5 s^{-1} for $NI^{\bullet-}$-C8-$PTZ^{\bullet+}$, $NI^{\bullet-}$-C11-$PTZ^{\bullet+}$, and $NI^{\bullet-}$-O-$PTZ^{\bullet+}$, in acetontrile respectively, which is assigned to the intermolecular charge recombination process of $NI^{\bullet-}$-L-PTZ and NI-L-$PTZ^{\bullet+}$, generated respectively from the bimolecular charge shift reaction between $NI^{\bullet-}$-L-$PTZ^{\bullet+}$ and NI-L-PTZ, because the slower components show the concentration dependence.

Although no NI(T_1) was observed in NI-L-PTZ dyads in acetonitrile, NI(T_1) was produced and observed in toluene. In toluene, the ϕ_f, τ_f, and ϕ_T of NI-L-PTZ dyads were smaller than those for the reference NI molecules. Therefore, the charge transfer process in toluene is the main deactivation process of NI(S_1) in NI-L-PTZ. It is clear that the electron transfer in NI-L-PTZ occurs only through NI(S_1) in toluene for the following reason. From the 30 ps transient absorption measurement of NI-L-PTZ, the transient absorption bands of $NI^{\bullet-}$ and $PTZ^{\bullet+}$ were observed immediately after the 355 nm excitation with 30 ps laser pulse. Because the generation of radical ions in the subnanosecond time scale was not observed in our 30 ps pump−probe experiments, the charge transfer process proceeds in a time scale significantly shorter than a few hundreds picoseconds. On the other hand, the charge recombination rates (k_{CR}) were estimated to be 3.6×10^8, 5.2×10^8, and 1.1×10^9 s^{-1} for $NI^{\bullet-}$-C8-$PTZ^{\bullet+}$, $NI^{\bullet-}$-C11-$PTZ^{\bullet+}$, and $NI^{\bullet-}$-O-$PTZ^{\bullet+}$, respectively.

Driving Force for Photoinduced Electron Transfer in NI-L-PTZ. The ΔG_{et} values for the electron transfer from an electron donor to an electron acceptor in the excited state were evaluated using:[26]

$$\Delta G_{et} = (E^0_{ox} - E^0_{red}) - E_{00} - \frac{e^2}{\epsilon R_{DA}} + e^2\left(\frac{1}{2r_D} + \frac{1}{2r_A}\right)\left(\frac{1}{\epsilon} - \frac{1}{\epsilon_{sp}}\right) \quad (1)$$

where E^0_{ox} and E^0_{red} are oxidation and reduction potentials for donor (D) and acceptor (A) molecules, respectively, and E_{00} denotes the excitation energy. $e^2/\epsilon R_{DA}$ is the Coulombic term, e is the charge of the electron, R_{DA} is the distance between D and A, r_D and r_A are the ionic radii of D and A, respectively, ϵ_{sp} is static dielectric constant of the high polar solvent in which the redox potentials are determined, and ϵ is the static dielectric constant of the low polar solvent. The ΔG_{et} values for the photoinduced electron transfer of NI-L-PTZ can be estimated from the reported reduction potential of NI (−1.44 V vs SCE)[20] and the oxidation potential of PTZ (0.67 V vs SCE).[27] The excitation energy of NI(S_1) was determined to be 3.40 eV from the intersection point of the absorption and fluorescence spectra of NI.[20,23,25] The excitation energy of NI(T_1) is well established to be 2.3 eV on the basis of the phosphorescence studies.[12,20] In the evaluation of ΔG_{et} values, we have used 9.35 and 7.20 Å for $2r_D$ and $2r_A$, respectively, which are obtained using the energy-minimized geometry by the semiempirical calculation (PM3 method) (Figure 6). R_{DA} was calculated to be 14.5, 16.9, and 17.5 Å for NI-C8-PTZ, NI-C11-PTZ, and NI-O-PTZ, respectively, by the same calculation based on the ground-state structures of NI-L-PTZ. Resulting ΔG_{et} values on the electron transfer from PTZ to NI(S_1) in NI-L-PTZ are listed in Table 3, showing the negative values in all solvents. This implies that the exergonic electron transfer can occur in NI(S_1)-L-PTZ to give $NI^{\bullet-}$-L-$PTZ^{\bullet+}$ in all solvents. On the other hand, the ΔG_{et} values show that the electron transfer from PTZ to NI(T_1) in NI(T_1)-L-PTZ can occur only in acetonitirle.

The relation between the excitation energies of NI(S_1) and NI(T_1) and the charge transfer (CT) states helps us to understand the charge transfer process of NI-L-PTZ. The energy levels for the low-lying $NI^{\bullet-}$-L-$PTZ^{\bullet+}$ radical ion pair states are shown in Figure 7. The energy of the CT state of $NI^{\bullet-}$-O-$PTZ^{\bullet+}$ becomes relatively higher than those of $NI^{\bullet-}$-C8-$PTZ^{\bullet+}$ and $NI^{\bullet-}$-C11-$PTZ^{\bullet+}$ in each solvent, because of the larger R_{DA} value in $NI^{\bullet-}$-O-$PTZ^{\bullet+}$ than in $NI^{\bullet-}$-C8-$PTZ^{\bullet+}$ and $NI^{\bullet-}$-C11-$PTZ^{\bullet+}$. It is important to note that these calculations are based on the assumption that dyads have linear structures, and that their geometries are unaffected by the charge transfer. The energy levels of the CT states are strongly affected by the solvent polarity. In acetonitrile, the CT states of three dyads lie below NI(S_1) and NI(T_1). However, in toluene or *n*-hexane, the CT states of dyads are located above NI(T_1), but below NI(S_1). Under this circumstance, the charge transfer from PTZ to NI(T_1) cannot occur in NI-L-PTZ. Actually, the transient absorption of $NI^{\bullet-}$ and $PTZ^{\bullet+}$ in toluene solutions can be observed

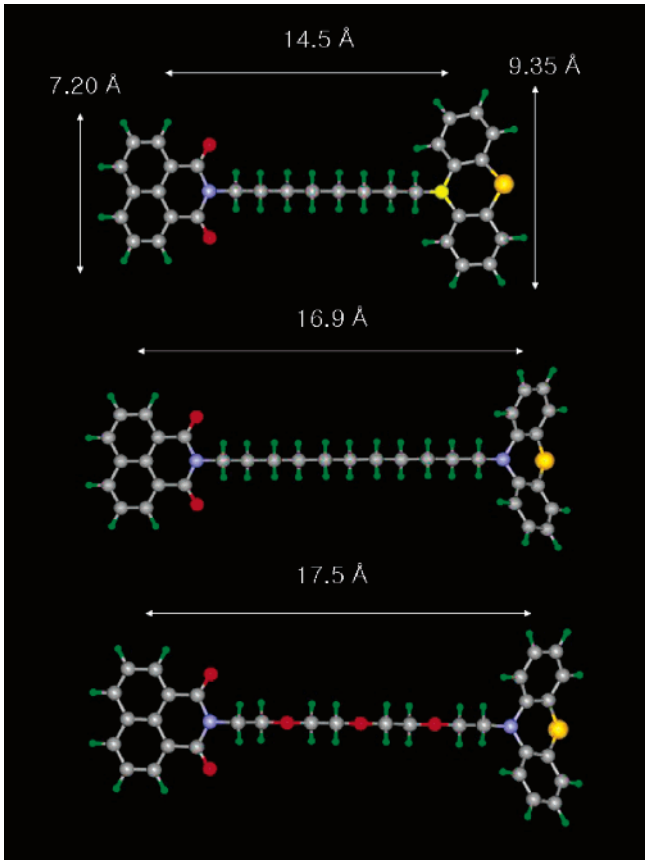

Figure 6. Optimized structures of NI-C8-PTZ, NI-C11-PTZ, and NI-O-PTZ using the semiempirical calculation (PM3 method). The geometric parameters were used for calculations of the energies of CT state and ΔG_{et} values.

TABLE 3: ΔG_{et} (eV) Values for the Charge Transfer from PTZ to NI(S_1) or NI(T_1) in NI-L-PTZ in Three Solvents

	in acetonitrile		in toluene		in *n*-hexane	
NI-L-PTZ	S_1	T_1	S_1	T_1	S_1	T_1
NI-C8-PTZ	−1.32	−0.22	−0.31	0.79	−0.04	1.06
NI-C11-PTZ	−1.31	−0.21	−0.25	0.85	−0.05	1.15
NI-O-PTZ	−1.31	−0.21	−0.24	0.86	0.05	1.15

within a few hundred picoseconds during the picosecond-laser photolysis experiment, indicating the absence of CT from NI(T_1).

We have considered the CT state of various conformers, because the present linker allows a lot of conformers. For example, R_{DA} values between NI and PTZ in folded conformers were calculated to be 5.35, 5.32, and 6.02 Å for NI-C8-PTZ, NI-C11-PTZ, and NI-O-PTZ, respectively, by the same PM3 calculation. In these cases, the energies of the CT state of the folded conformers become lower than those of linear structures. Even in toluene and *n*-hexane, the CT states still lie between NI(S_1) and NI(T_1). Thus, the conformers do not induce CT mechanism change in the present dyads.

Effects of Linker on Photoinduced Electron Transfer in NI-L-PTZ. No effect of the linkers was found on the properties of NI-L-PTZ in the ground state, because the steady-state absorption and fluorescence spectra were almost equivalent for three dyads in three solvents. Similar τ_f and ϕ_f values and no formation of NI(T_1) were shown in acetonitrile and *n*-hexane, but relatively efficient formation of NI(T_1) with $\phi_T = 0.23$ was found for NI-L-PTZ in toluene (Table 1).

Both $\phi_{NI^{\bullet-}}$ and $\phi_{PTZ^{\bullet+}}$ values in acetonitrile were almost equivalent for NI-L-PTZ. The rate constants of the charge

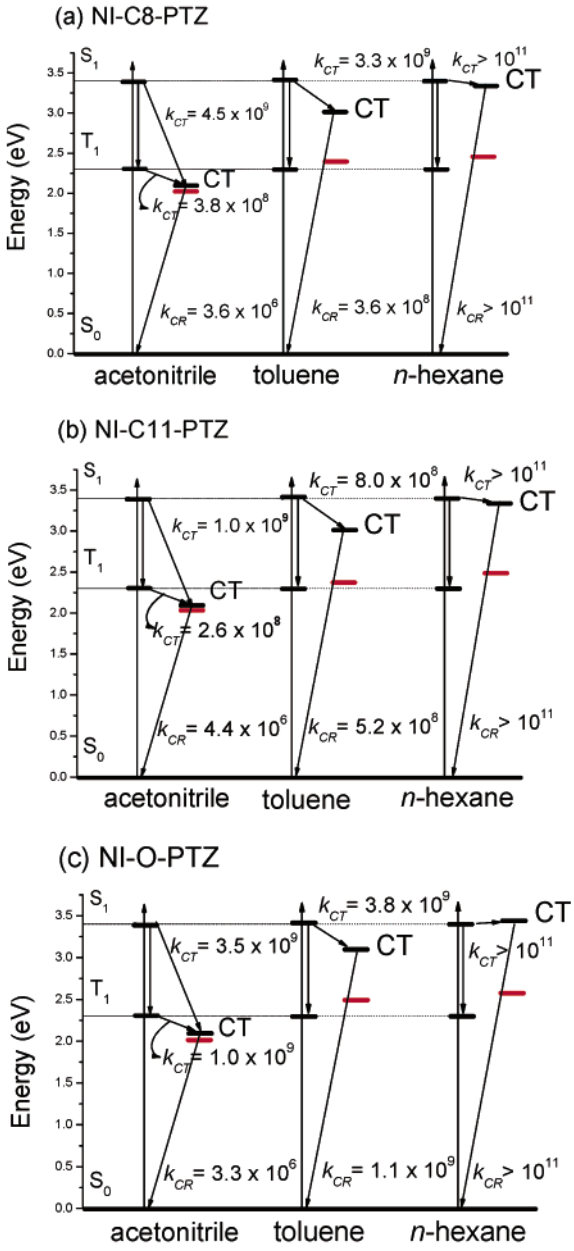

Figure 7. Schematic diagram of charge transfer process following photoexcitation of NI-C8-PTZ (a), NI-C11-PTZ (b), and NI-O-PTZ (c) in various solvents. The charge transfer state (CT) was calculated using the spectroscopic method, which is based on Weller's dielectric continuum treatment for the energy of CT in an arbitrary solvent. k_{CT} and k_{CR} are the charge transfer rate and the charge recombination rate, respectively. The CT states were denoted corresponding to the extended conformers (black line) and the folded conformers (red line), respectively.

transfer process (k_{CT}) were found to be enhanced in NI-O-PTZ 3−5 times compared with those in NI-C11-PTZ. It is well-known that polyether linkers accelerate the charge transfer and charge recombination through the superexchange mechanism, compared with polymethylene linkers, because of the more efficient electronic coupling between the donor and acceptor through polyether linkers than through polymethylene linkers. On the other hand, the k_{CT} value of NI-C8-PTZ was larger than that of NI-C11-PTZ, which is due to the shorter distance between electron donor and acceptor moieties in NI-C8-PTZ than in NI-C11-PTZ.

In acetonitrile, the charge recombination between $NI^{\bullet-}$ and $PTZ^{\bullet+}$ could be controlled by the polar solvent, resulting in

observations of similar k_{CR} values for NI-L-PTZ. However, the highly fast charge recombination between $NI^{\bullet-}$ and $PTZ^{\bullet+}$ in $NI^{\bullet-}$-L-$PTZ^{\bullet+}$ in toluene can be explained by involvement of $NI(T_1)$ lying below the CT state, as shown in Figure 7, if the intersystem crossing from the CT state to $NI(T_1)$ is efficient. Furthermore, the fast charge recombination in toluene could be ascribed by the close interaction between $NI^{\bullet-}$ and $PTZ^{\bullet+}$ moieties, which can be achieved in nonpolar toluene compared to polar acetonitrile. Moreover, the higher k_{CR} of NI-O-PTZ compared with those of NI-C8-PTZ and NI-C11-PTZ reveals that the electronic coupling through polyether linkers can also enhance the charge recombination process in toluene.

Exciplex Formation between NI(S_1) and Toluene. Wintgen et al.[20] suggested that because an upper triplet excited state, $NI(T_2)$ with n,π^* character, is energetically close to $NI(S_1)$ with π,π^* character for NI derivatives, the solvent induces the substantial effects on the deactivation process of $NI(S_1)$. In polar solvents, the energy gap between $NI(S_1)$ and $NI(T_2)$ increases and mixing of $NI(S_1)$ and $NI(T_2)$ is less important; as a consequence, both τ_f and ϕ_f are large. On the other hand, in nonpolar solvents, the fastest intersystem crossing process occurs from $NI(S_1)$. Previous studies reported that τ_f and ϕ_f of $NI(S_1)$ of NI derivatives have their lowest values in nonpolar solvents.[20] A similar trend was clearly observed here for all NI derivatives that have τ_f shorter than 50 ps and ϕ_f smaller than 0.001 in *n*-hexane (Table 1).

Solvent plays a significant role in photophysical behaviors of NI in the excited states. Generally, the Stokes shift exhibits solvent effect as a function of the solvent polarity. Polarity dependent shifts in the absorption and fluorescence spectra are also common. NI derivatives in the lowest singlet excited state are known to show changes on moving from nonpolar to polar solvents in accordance with general solvent effect. Although the dielectric constant ($\epsilon = 2.38$) of toluene is comparable to that of *n*-hexane ($\epsilon = 1.89$), the fluorescence peak in toluene appeared at a wavelength longer than that in *n*-hexane or in acetonitrile. Furthermore, the vibrational structure of the fluorescence band was diminished. These may be attributed to the very specific solvent effects such as the exciplex formation. The τ_f values of the reference NI molecules in toluene are rather longer than those in acetonitrile, whereas the intersystem crossing efficiencies are approximately 50% of those in acetonitrile. Thus, the smaller ϕ_T values for the reference NI molecules in toluene can be explained on the basis of the exciplex formation with toluene.

Conclusions

We have carried out the transient absorption measurements to investigate the PET processes between $NI(S_1)$ or $NI(T_1)$ and PTZ in NI-L-PTZ. The large negative ΔG_{et} values for $NI(S_1)$ and $NI(T_1)$ clearly demonstrate that the electron transfer from the electron-donor PTZ moiety to the electron-acceptor $NI(S_1)$ or $NI(T_1)$ moiety is exergonic in acetonitrile, whereas it occurs through $NI(S_1)$, but not through $NI(T_1)$ in toluene. The difference corresponds to the CT state stabilized more in acetonitrile than in toluene because of the polar character of acetonitrile. The distinct k_{CT} value in NI-L-PTZ implies that the length of linkers and electronic coupling through the polyether linker affected to the CT process. It is found that the exciplex formation occurred between $NI(S_1)$ and solvent toluene.

Acknowledgment. This work has been partly supported by a Grant-in-Aid for Scientific Research (Project 17105005, Priority Area (417), 21st Century COE Research, and others) from the Ministry of Education, Culture, Sports, Science and Technology (MEXT) of the Japanese Government. U.C.Y. acknowledges the Korea Research Foundation (MOEHRD, Basic Research Promotion Fund RO5-2004-000-10557-0) for financial support.

Supporting Information Available: Transient absorption spectra for NI-C11-PTZ and reference NI molecules in acetonitrile and in toluene. Table of absorption and fluorescence maxima of NI derivatives in three solvents. This material is available free of charge via the Internet at http://pubs.acs.org.

References and Notes

(1) Wasielewski, M. R. *Chem. Rew.* **1992**, *92*, 435.
(2) Gust, D.; Moore, T. A.; Moore, A. L. *Acc. Chem. Res.* **1993**, *26*, 198.
(3) Le, T. P.; Rogers, J. E.; Kelly, L. A. *J. Phys. Chem. A* **2000**, *104*, 6778.
(4) Marcus, R. A. *Rev. Mol. Phys.* **1993**, *65*, 599.
(5) Bolton, J. R.; Archer, M. D. *Adv. Chem. Ser.* **1991**, *228*, 7.
(6) Kanoka, Y.; Sakai, K.; Murata, R.; Hatanaka, Y. *Heterocycles* **1975**, *3*, 719.
(7) Yoon, U. C.; Oh, S. W.; Lee, J. H.; Park, J. H.; Kang, K. T.; Mariano, P. S. *J. Org. Chem.* **2001**, *66*, 939.
(8) Yoon, U. C.; Jin, Y. X.; Oh, S. W.; Park, C. H.; Park, J. H.; Campana, J. H.; Cai, X.; Duesler, E. N.; Mariano, P. S. *J. Am. Chem. Soc.* **2003**, *125*, 10664.
(9) Saito, I.; Takayama, M.; Sugiyama, H.; Nakatani, K.; Tsuchida, A.; Yamamoto, M. *J. Am. Chem. Soc.* **1995**, *117*, 6406.
(10) Kawai, K.; Osakada, Y.; Takada, T.; Fujitsuka, M.; Majima, T. *J. Am. Chem. Soc.* **2004**, *126*, 12843.
(11) Takada, T.; Kawai, K.; Tojo, S.; Majima, T. *J. Phys. Chem. B* **2004**, *108*, 761.
(12) Jones II, G.; Kumar, S. *J. Photochem. Photobiol. A: Chem.* **2003**, *160*, 139.
(13) Barros, T. C.; Filho, B.; Toscano, V. G.; Politi, M. J. *J. Photochem. Photobiol. A: Chem.* **1995**, *89*, 141.
(14) Abraham, B.; Kelly, L. A. *J. Phys. Chem. B* **2003**, *107*, 12534.
(15) Cho, D. W.; Fujitsuka, M.; Choi, K. H.; Park, M. J.; Yoon, U. C.; Majima, *J. Phys. Chem. B* **2006**, *110*, 4576.
(16) Sakamoto, M.; Cai, X.; Hara, M.; Tojo, S.; Fujitsuka, M.; Majima, T. *J. Phys. Chem. A* **2004**, *108*, 8147.
(17) Fujitsuka, M.; Okada, A.; Tojo, S.; Takei, F.; Onitsuka, K.; Takahashi, S.; Majima, T. *J. Phys. Chem. B* **2004**, *108*, 11935.
(18) Murov, S. L.; Carmichael, I.; Hug, G. L. *Handbook of Photochemistry*, 2nd ed.; Marcel Dekker: New York, 1993.
(19) Carmichael, I.; Hug, G. *J. Phys. Chem. Ref. Data* **1986**, *15*, 54.
(20) Wintgens, V.; Valet, P.; Kossanyi, J.; Biczok, L.; Demeter, A.; Berces, T. *J. Chem. Soc., Faraday Trans.* **1994**, *90*, 411.
(21) Kawai, K.; Takada, T.; Tojo, S.; Majima, T. *Tetrahedron Lett.* **2002**, *43*, 89.
(22) Alkaitis, S. A.; Beck, G.; Graetzel, M. *J. Am. Chem. Soc.* **1975**, *97*, 5723.
(23) Rogers, J. E.; Kelly, L. A. *J. Am. Chem. Soc.* **1999**, *121*, 3854.
(24) Takada, T.; Kawai, K.; Fujitsuka, M.; Majima, T. *Proc. Natl. Acad. Sci. U.S.A.* **2004**, *101*, 14002.
(25) Rogers, J. E.; Weiss, S. J.; Kelly, L. A. *J. Am. Chem. Soc.* **2000**, *122*, 427.
(26) Weller, A. Z. *Z. Phys. Chem.* **1982**, *133*, 93.
(27) Lai, R. Y.; Fabrizio, E. F.; Lu, L.; Jenekhe, S. A.; Bard, A. J. *J. Am. Chem. Soc.* **2001**, *123*, 9112.